



International Congress of Science and Technology of Metallurgy and Materials, SAM - CONAMET 2013

## Properties of NiMnGa Alloys Ultra Rapidly Solidified by Suction Casting

Esteban Rodoni<sup>a</sup>, Jorge M. Levingston<sup>b,c</sup>, Sebastián Deghi<sup>c</sup>, Daniel E. Lescano<sup>c</sup>, Gabriela Pozo López<sup>b,c</sup>, Silvia E. Urreta<sup>c</sup>, Luis M. Fabietti<sup>b,c\*</sup>

<sup>a</sup>*Instituto Sábató, Universidad de San Martín, San Martín, Buenos Aires, Argentina.*

<sup>b</sup>*Instituto de Física Enrique Gaviola. CONICET, Córdoba, Argentina.*

<sup>c</sup>*Facultad de Matemática, Astronomía y Física, Universidad Nacional de Córdoba. Córdoba, Argentina.*

### Abstract

Ni<sub>2</sub>MnGa alloys are obtained by suction casting in water chilled cylindrical copper moulds 50 mm long and 1-4 mm in diameter; the microstructure and the magnetic properties are then investigated as functions of the cylinder diameter. The solidification substructures are characterized by scanning electron microscopy and confocal microscopy. The martensitic transformation temperatures, determined by magnetization vs. temperature measurements, are lower than those measured in bulk Ni<sub>2</sub>MnGa single crystals (202 K). The demagnetization curves measured from saturation in the martensitic state show two steps: the first is at about +130 mT and the larger second one at relatively large inverse fields (about -300 mT), except in cylinders 4 mm in diameter, where these steps overlap at low inverse fields. These steps are likely to arise from a demagnetization mechanism involving field induced twin boundary motion in a few martensite variants, indicating a ferromagnetic shape memory effect in the cylinders.

© 2015 The Authors. Published by Elsevier Ltd. This is an open access article under the CC BY-NC-ND license (<http://creativecommons.org/licenses/by-nc-nd/4.0/>).

Selection and peer-review under responsibility of the scientific committee of SAM - CONAMET 2013

**Keywords:** Ni<sub>2</sub>MnGa alloy; Ultra rapid solidification; Magnetic shape memory; Martensitic transformation.

### 1. Introduction

Ferromagnetic shape memory alloys are active materials which may undergo relatively large magnetic field

\* Corresponding author. Tel.: +54-351-433-4051; fax: +54-351-433-4054.

E-mail address: [fabietti@famaf.unc.edu.ar](mailto:fabietti@famaf.unc.edu.ar)

induced strains, associated to twin boundary movements in the martensitic phase. These magnetic shape memory materials have been largely investigated because of their high potential in the design of fast actuating devices and sensors [Kainuma et al. (2006); Dunand and Müllner (2011)]. In 1996 K. Ullako et al. [Ullako et al. (1996)] reported this phenomenon for the first time in stoichiometric  $\text{Ni}_2\text{MnGa}$  alloys; more recently, strains about 10% have been obtained for magnetic fields about 1T, in unstressed single crystals of this material in the orthorhombic  $7M$  martensitic phase [Sozinov et al. (2002)].

During cooling from the melt, the  $\text{Ni}_2\text{MnGa}$  alloy undergoes different transformations: an ordering transition ( $B2$  to  $L2_1$ ) at high temperature, a ferromagnetic transformation and also a structural martensitic transformation [Vasil'ev et al. (1999)]. In this alloy, the martensitic temperature is below the Curie temperature so this transformation involves two different ferromagnetic phases. Both transformation temperatures are strongly sensitive to the alloy composition.

The magnetic-field-induced strain is due to twin boundaries moving under the influence of an internal stress produced by the magnetic anisotropy energy; in general, this strain is not recovered upon field removal, as observed with the true plastic strain produced by twin boundary motion induced by an externally applied stress in nonmagnetic shape-memory alloys.

The magnetoplastic strains in polycrystalline magnetic shape memory alloys, with no mechanical bias stress applied, are negligibly small as compared to those found in single crystals. However, relatively large magnetic field induced shape memory effects have been reported in melt spun polycrystalline ribbons [Enkovaara et al. (2004), Murray et al. (2000), Müllner et al. (2002)]. In fact, melt spinning is an effective way to produce textured, small grained polycrystalline ribbons of ferromagnetic shape memory alloys; when compared with the as-cast master alloy, the as-quenched ribbons exhibit a lower martensitic transformation temperature  $T_M$  and Curie temperature  $T_C$ , and a reduced saturation magnetization  $M_S$ . The melt spun polycrystalline Ni-Mn-Ga ribbons exhibit in the as-cast condition, and even after annealing at temperatures below 773 K, a marked step in the  $M(H)$  hysteresis loops [Wang et al. (2009); Pozo López et al. (2013); Wang et al. (2013)], which has been attributed to magnetic field induced twin boundary motion (MFITBM), in the particular scenario of texture and quenched-in internal stresses, built up during solidification onto the rotating copper wheel.

Another ultra rapid solidification method inducing large crystallographic textures and residual internal stresses is suction casting [Pawlick et al., 2008], in which a large pressure difference forces the melt alloy into a water chilled copper mould. With this technique, bulk samples can be obtained with really high textures.

This article reports our first results on the microstructure and the magnetic properties of  $\text{Ni}_2\text{MnGa}$  alloys processed by suction casting to obtain cylinders 1-4 mm diameters; special attention is paid to the martensitic transformation at low temperature and to evidences of MFITBM in the martensitic phase.

## 2. Experimental procedures

A master alloy of nominal composition  $\text{Ni}_2\text{MnGa}$  was prepared by arc melting 99.9 % Ni (Strem Chemicals), 99.95 % Mn (Alfa Aesar) and 99.99 % Ga (Strem Chemicals); the small ingots so obtained (about 5 g) were further re-melted four times to promote an homogeneous distribution of the components. All these procedures were conducted under a Zr gettered Ar atmosphere. The alloy was further processed by suction casting into cylindrical bulk pieces 1mm–4 mm diameter and 50 mm length. The solidification microstructure of the as-cast samples was characterized by confocal microscopy and by scanning electron microscopy (SEM) in a FE SEM Zeiss microscope. Samples for electron microscopy were mechanically polished only while for confocal microscopy they were further etched in a solution of 2% vol. (methyl alcohol 98vol%- nitric acid 2vol%), for 2 s at 293 K.

Magnetic hysteresis loops were measured in a vibrating sample magnetometer (VSM) Lakeshore 7300, with a maximum field up to 1 T.

## 3. Results and Discussion

### 3.1. Microstructure

The resulting solidification microstructures, observed by confocal microscopy, are shown in Fig. 1 to Fig.4. All the samples exhibit columnar grains developed in the radial direction, as expected for the heat extraction geometry

imposed during cooling. Fig. 1.a shows a transversal cut corresponding to a 1mm diameter cylinder. Inside the grains, dark contrast lines are observed, also following the radial direction, as shown at a higher magnification in Fig. 1.b, which corresponds to the area indicated by the rectangle in 1.a. Compositional profiles were measured along lines normal to the dark lines in Fig.1.b but no segregation could be detected; instead, a uniform composition close to the nominal value was measured.

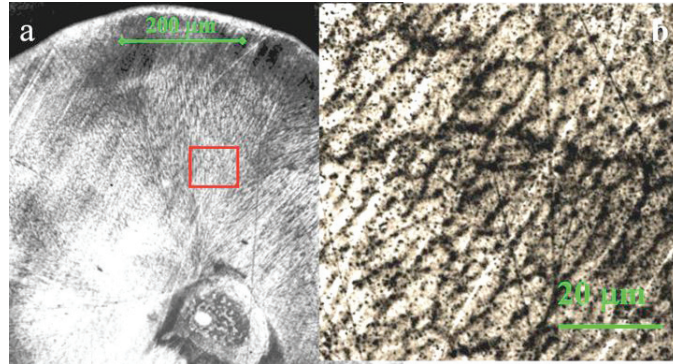


Fig. 1. Confocal micrograph of a transversal surface of sample 1 mm diameter, normal to the cylinder length showing, (a) the radial grain structure and (b) an enlarged image of the area indicated by the rectangle in (a). The contrast observed could not be associated to segregation.

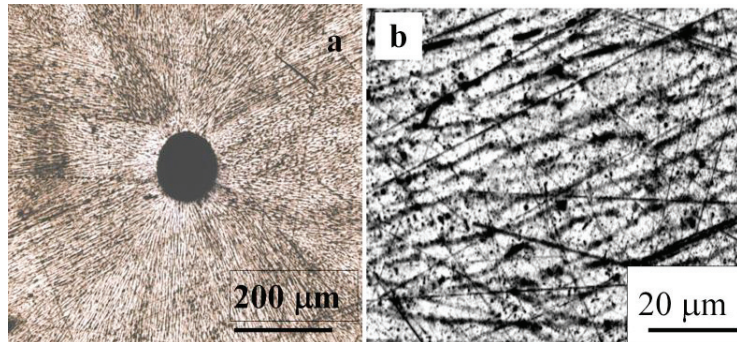


Fig. 2. Confocal micrograph of a transversal surface of sample 2 mm diameter, normal to the cylinder length showing, (a) the radial grain structure and (b) an enlarged image of the thin contrast lines observed in (a). This sample has a hollow cylindrical core in the centre. As before, the contrast observed could not be associated to segregation.

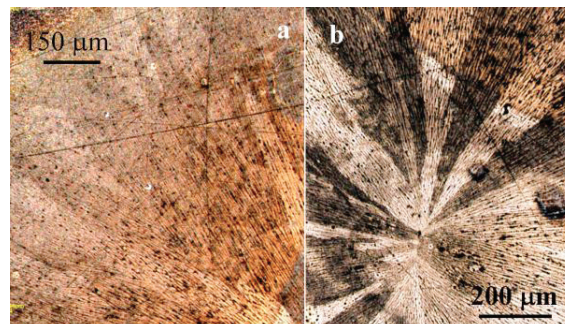


Fig.3. Confocal micrograph of a transversal surface of sample 3 mm diameter, normal to the cylinder length showing, the radial grain structure near the external surface (a) and in the center (b); in both zones thin contrast lines along the diameter direction are observed.

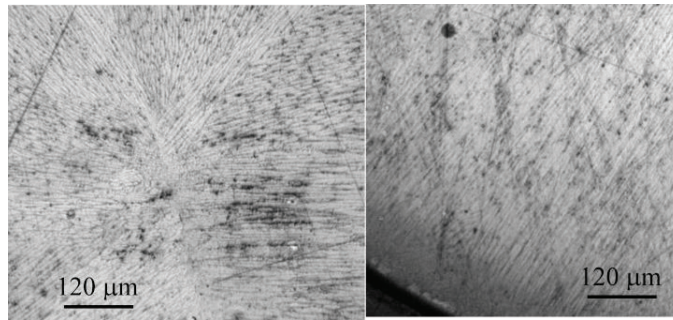


Fig.4. Confocal micrograph of a transversal surface of sample 4 mm diameter, showing radial grain structure in the center (left) and near the external surface (right); in both zones thin contrast lines along the diameter direction are observed.

Similar micrographs are shown for cylinders 2mm diameter in Fig. 2. These samples exhibit a hollow core (they actually are tubes with quite wide walls) and also show columnar grains radially oriented. Again, dark lines are observed inside the grains, parallel to the radius direction - Fig. 2.b - which could not be associated with any local segregation process.

Similar features are displayed in Fig. 3 and Fig. 4 for cylindrical samples 3 mm and 4 mm in diameter. These relatively thick samples also show two slightly different contrasts: in the outer zone, close to the surface and in the central zone, where the different grains converge. No composition changes could be detected along the grain axis nor in the perpendicular direction, as illustrated in Fig. 5 for sample 3mm diameter; in this figure the sample is polished but not etched and the dark and clear band contrast corresponds to different grains in the outer region, close to the cylinder surface.

Table 1. Temperatures corresponding to the onset ( $M_s$ ) and to the end ( $M_f$ ) of the austenite to martensite transformation during cooling and to the onset and the end of the martensite to austenite back transformation, taking place during heating, as calculated by the method illustrated in Fig.7.

Diameter [mm]	$[M_s \pm 1]$ [K]	$[M_f \pm 1]$ [K]	$[A_s \pm 1]$ [K]	$[A_f \pm 1]$ [K]
1	142	126	156	175
2	130	110	141	166
3	145	131	158	174
4	146	132	155	171

As shown in Fig. 5 no significant composition changes could be detected, confirming that the fine contrast observed is not related to composition inhomogeneities, arising in segregation during the ultra rapid solidification process imposed to these samples. Concerning the dark precipitate-like spots observed in Fig. 5, it is found that the matrix is locally depleted of the three major elements, Ni, Mn and Ga leading to conclude that they actually are small pores. Summarizing the microstructure results they indicate that this solidification process promotes quite large crystallographic textures without any appreciable segregation.

### 3.2. The martensitic transformation

The magnetic polarization versus temperature is investigated in the range between 10K and 300 K, where the martensitic transformation is expected to take place (Fig. 6). The transformation temperatures  $M_S$  and  $M_F$  corresponding to the *onset* and the *final* of the martensitic transformation during cooling, and  $A_S$  and  $A_F$  the initial and final temperatures associated to the transformation to the austenitic phase during heating are estimated as



illustrated in Fig.7. The values resulting from data shown in Fig.6 are listed in Table 1. On the basis of these values it may be concluded that the transformation temperatures are not correlated with the sample diameter. On the other hand, these results are consistent with a uniform composition throughout the samples. No evidence of any pre-martensitic transformation could be observed as previously found for this magnetization based detection technique [Zheludev et al. (1995)].

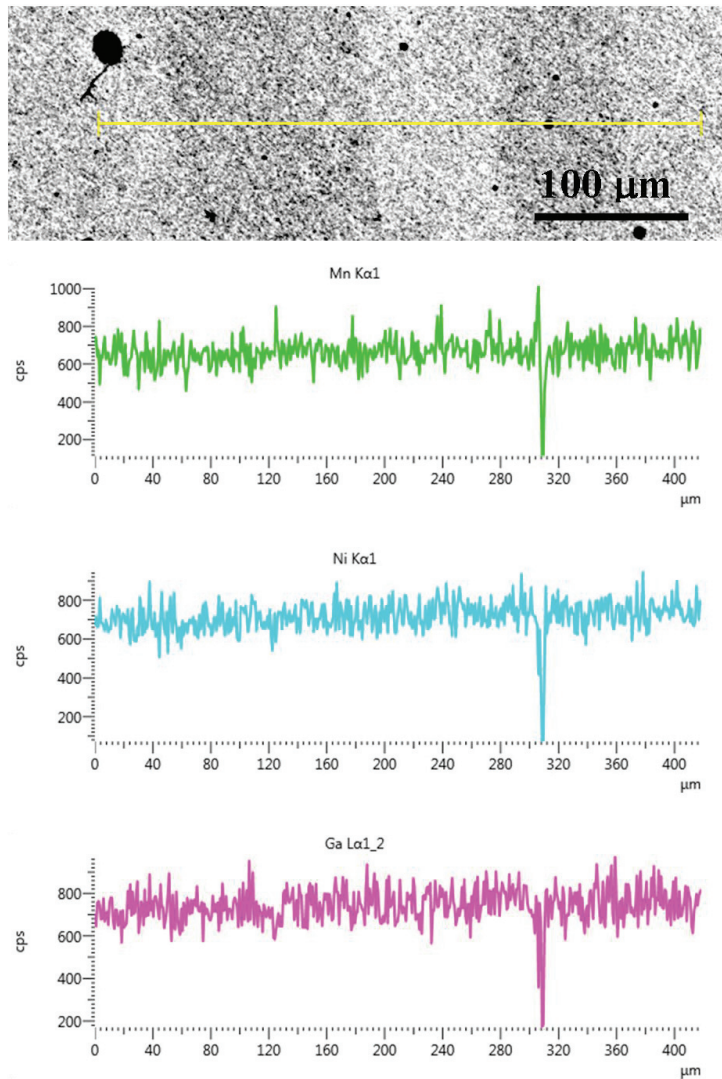


Fig.5. EDS compositional profiles corresponding to Mn, Ni and Ga along a line crossing three grain boundaries in cylinder 3 mm diameter. The observed contrast seems not associated to different composition. Small black circles are not precipitates but round pores.

The values in Table 1 are lower than those measured in bulk  $\text{Ni}_2\text{MnGa}$  alloys ( $T_M=202\text{ K}$ ) [Webster et al. (1984)]. This reduction in the martensitic transformation temperature is likely due to disorder certainly present in small grained, textured and stressed samples; disorder enhances the resistance to the transformation and lowers the martensitic transformation temperature [Guo et al. (2005)].

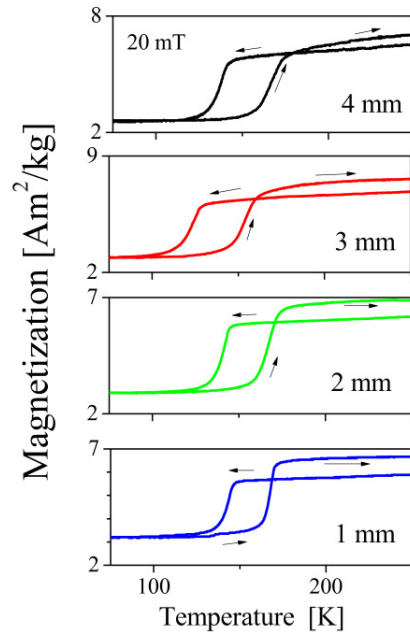


Fig. 6. Magnetization vs. temperature curves corresponding to the different cylinders investigated. They were measured under an applied field of 20 mT. From these curves the values quoted in Table 1 are obtained following the procedure indicated in Figure 7.

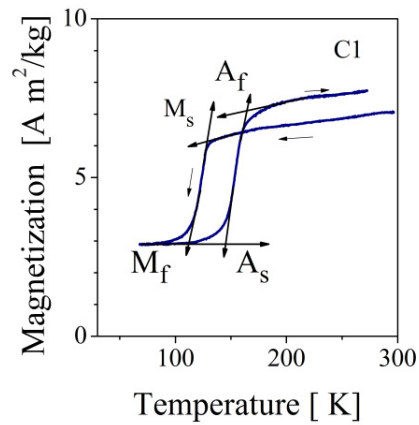


Fig.7. Magnetization vs. temperature curve measured for the 1 mm diameter cylinder is plotted to illustrate the procedure used to define the transformation temperatures.

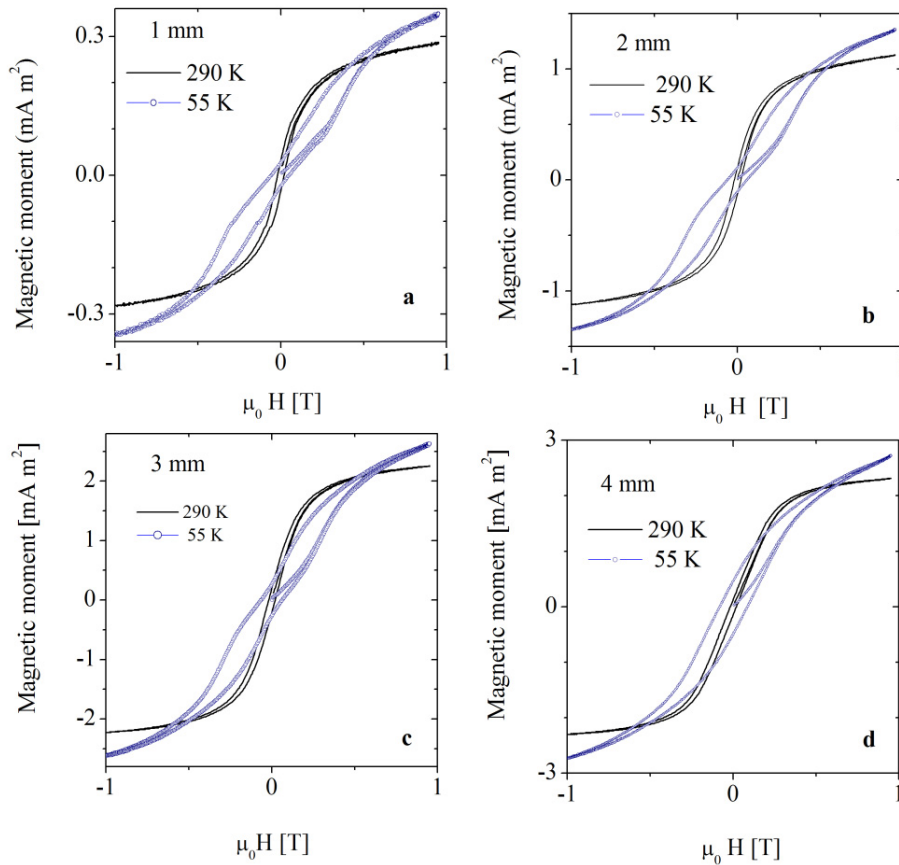


Fig. 8. Hysteresis loops measured with the sample in the austenitic phase (290 K) and at a low temperature (55 K) at which it has completely transformed to martensite. In the austenitic phase, cylinders are magnetically soft while at low temperature they show the characteristic features of a magnetization mechanism involving field induced twin boundary motion.

### 3.3. Magnetic properties

The isothermal hysteresis loops measured at two different temperatures, 290 K in the range of the austenitic high temperature phase and another one at 55 K, where the transformation is complete, are shown in Fig. 8 for the microstructures investigated. It is worth to note that *two* distinct peaks are detected in the differential susceptibility during demagnetization of the martensitic phase from saturation - see Fig. 9 -; the first maximum in the  $\chi(H)$  plot (first step in the demagnetization curve) appears at a positive (first quadrant) internal field (about 130 mT) while another maximum is observed at about -300 mT. This hysteresis loop behavior is completely reproducible during subsequent field cycles. The largest step has already been observed [Wanget al. (2009), Pozo López et al. (2013), Wang et al. (2013)] in Ni-Mn-Ga polycrystalline melt spun ribbons, and it was attributed to magnetic field induced twin boundary motion (MFITBM) in the martensitic phase.

The phenomenon is explained on the basis of the ribbon crystallographic texture and the internal stresses built up during quenching [Wang et al. (2009), Wang et al. (2013)], which induce the cubic austenite to transform into a few twin variants of orthorhombic martensite during cooling. The abrupt slope change in the martensite  $M(H)$  curves

would correspond to the onset of MFITBM in the preferentially oriented martensite. The restoring 'force' leading to reversible twin boundary motion is proposed to be the grain-to-grain elastic energy stored in the polycrystalline sample. In the present case it is not possible to describe the actual mechanism leading to magnetic shape memory, but it is likely that the large peaks in the  $\chi(H)$  curves are related to the special texture and quenched-in stresses present in our samples.

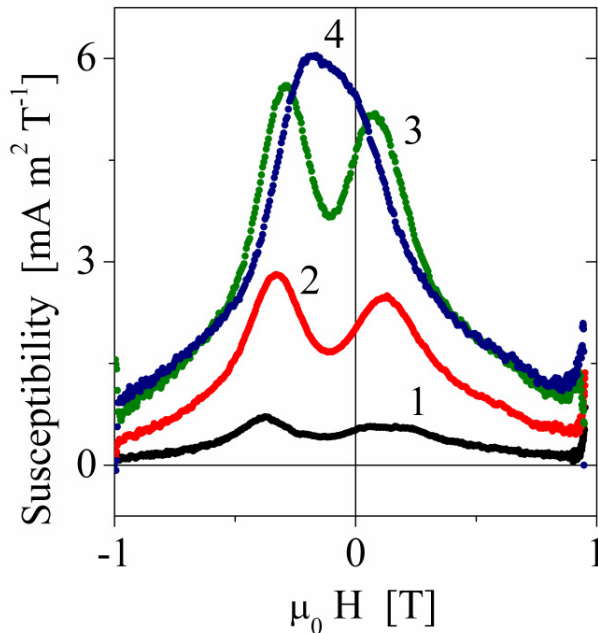


Fig. 9. Differential susceptibility ( $\frac{\partial M}{\partial H}$ ) corresponding to the low temperature loops in Figure 8. Two susceptibility peaks are observed, except for the cylinder 4 mm diameter for which these peaks seem to overlap. This behaviour is at present not well understood.

#### 4. Conclusions

Ni<sub>2</sub>MnGa cylinders (50 mm long) are produced by suction casting with four different diameters (1 mm to 4 mm) to explore the effects of an ultra fast quenching condition on the alloy microstructure and magnetic properties, in particular the ferromagnetic shape memory ability.

Samples are polycrystalline, with radial columnar grains leading to a large crystallographic texture. The alloy composition, on the other hand is quite uniform, with no evidence of segregation even in samples 4 mm diameter, undergoing the lowest cooling rate.

The austenitic and the martensitic phases are ferromagnetic; the austenitic phase exhibits a very low coercivity, near 4 mT while the martensite hysteresis loops exhibit larger coercivity and remanence values. The low temperature hysteresis loops, corresponding to the martensitic phase, show similar features as those reported by other authors in melt spun Ni-Mn-Ga ribbons as indicative of a magnetization process involving magnetic field induced twin boundary motion. The demagnetization curves measured from saturation in the martensitic state show *two* marked steps: a first one for positive fields (~ 130 mT) and a larger second one for relatively large inverse fields (~ 300 mT) in all the samples. These steps tend to overlap in samples with the largest radius giving a single, broad peak near  $H=0$ .

Even when these samples must be further investigated and the actual low temperature magnetization mechanism



must be precisely characterized, this processing route seems promising to obtain polycrystalline bulky pieces of this alloy exhibiting ferromagnetic shape memory properties.

## Acknowledgements

This work was supported in part by CONICET and SECyT-UNC, Argentina.

## References

- Dunand, D.C., Müllner, P., 2011, Size effects on magnetic actuation in Ni-Mn-Ga shape-memory alloy. *Adv. Mater.* 23, 216-232.
- Enkovaara, J., Ayuela, A., Zayak, T., Entel, P., Nordström, L., Dube, M., J. Jalkanen, J. Impola, R. M. Nieminen. Magnetically driven shape memory alloys, *Mater. Sci. Eng. A*, 378 (2004) 52–60.
- Guo, S., Zhang, Y., Li, J., Quan, B., Qi, Y., Wang, X., 2005 Martensitic transformation and magnetic-field-induced strain in magnetic shape memory alloy NiMnGa melt-spun ribbon. *J. Mater. Sci. Technol.* 21, 211- 214.
- Kainuma, R., Imano, Y., Ito, W., Sutou, Y., Morito, H., Okamoto, S., Kitakami, O., Oikawa, K., Fujita, A., Kanomata, T., Ishida, K., 2006, Magnetic-field-induced shape recovery by reverse phase transformation. *Nature (London)* 439, 957-960.
- Murray, S.J., Marioni, M., Allen, S.M., O’Handley, R.C., Lograsso, T.A., 2000, 6% magnetic-field-induced strain by twin-boundary motion in ferromagnetic Ni–Mn–Ga. *Appl. Phys. Lett.* 77 886-888.
- Müllner, P., Chernenko, V.A., Wollgarten, M., Kostorz, G., 2002, Large cyclic deformation of a Ni-Mn-Ga shape memory alloy induced by magnetic fields, *J. Appl. Phys.* 92, 6708-6713.
- Pawlick, P., Pawlick, K., Przibil, A. Investigation of the cooling rate in the suction casting process, *Re. Adv. Mater. Sci.* 18 (2008) 81-84.
- PozoLópez, G., Condó, A.M., Giordano, R.N., Urreta, S.E., Haberkorn, N., Winkler, E., Fabietti, L.M., 2013, Microstructure and magnetic properties of as-cast Ni<sub>2</sub>MnGa alloys processed by twin roller melt spinning, *J. Magn. Magn. Matter.* 335, 75–85.
- Sozinov, A., Likhachev, A.A., Lanska, N., Ullakko, K., 2002, Giant magnetic-field-induced strain in NiMnGa seven-layered martensitic phase. *Appl. Phys. Lett.* 80 (10), 1746-1748.
- Takagi, T., Tani, J., 1999, Structural and magnetic phase transitions in shape-memory alloys Ni<sub>2-x</sub>Mn<sub>1-x</sub>Ga. *Phys. Rev. B* 59 (2), 1113-1120.
- Ullakko, K., Huang, J. K., Kantner, C., O’Handley, R.C., Kokorin, V.V., 1996, Large magnetic-field-induced strains in Ni<sub>2</sub>MnGa single crystals. *Appl. Phys. Lett.* 69 (13), 1966-1968.
- Vasil’ev, A.N., Bozhko, A.D., Khovailo, V.V., Dikshtein, I.E., Shavrov, V.G., Buchelnikov, V.D., Matsumoto, M., Suzuki, S., Wang, J., Jiang, C., Techapiesanchaorenkij, R., Bono, D., Allen, S.M., O’Handley, R.C., 2009, Anomalous magnetizations in melt spinning Ni–Mn–Ga. *J. Appl. Phys.* 106, 023923-1-3.
- Wang, J., Jiang, C., Techapiesanchaorenkij, R., Bono, D., Allen, S.M., O’Handley, R.C., 2013, Microstructure and magnetic properties of melt spinning Ni-Mn-Ga, *Intermetallics* 32 151-155.
- Webster, P.J., Ziebeck, K.R.A., Town, S.L., Peak, M.S., 1984, Magnetic Order and Phase Transformation in Ni<sub>2</sub>MnGa, *Philos. Mag. B* 49 295-310.
- Zheludev, A., Shapiro, S.M., Wochner, P., Schwartz, A., Wall, M., Tanner, L.E., 1995, Phonon anomaly, central peak, and microstructures in Ni<sub>2</sub>MnGa, *Phys Rev B* 51, 11310-14.